

The Hamburg Quasar Monitoring Program (HQM) at Calar Alto*

I. Low amplitude variability in quasars

U. Borgeest and K.-J. Schramm

Hamburger Sternwarte, Gojenbergsweg 112, D-W 2050 Hamburg 80, Germany

Received date; accepted date

Abstract. HQM is an optical broad-band photometric monitoring program carried out since Sept. 1988. Our main intention is to search for indications of microlensing in a sample of ~ 100 selected quasars; however, we also want to study the intrinsic variability. We use a CCD camera equipped to the MPIA 1.2 m telescope. Fully automatic photometric reduction relative to stars in the frame is done within a few minutes after each exposure, thus interesting brightness changes can be followed in detail. The typical photometric error is 1–2% for a 17.5 mag quasar, making HQM the most accurate long-term quasar monitoring program yet carried out. The main results of HQM which we discuss here are: (1) Concerning variability, quasars form two, clearly distinct classes, optically violent variables (OVVs) and non-OVVs. (2) All OVVs are radio loud and probably belong to the blazar class. (3) Non-OVVs have lightcurve gradients of at most several 0.1 mag yr^{-1} in the quasar restframe and can be well fitted by polynomials of low order. (4) Although our data cover only a relatively short timespan, we conclude that there is a large fraction of quasars which would be undetectable in photographic surveys using optical variability alone as the selection criterium. (5) A broad class of flat-spectrum radio quasars are no blazars, they are even less variable in the optical than radio quiet objects. (6) There is some statistical evidence for microlensing in our sample; if present it does, however, lead only to low lightcurve gradients.

Key words: Techniques: photometric – quasars: general – gravitational lenses

1. Introduction

For the HQM program (e.g. Borgeest et al. 1991a,b; Borgeest & Schramm 1992; Schramm & Borgeest 1992; v. Linde et al. 1993; Schramm et al. 1993a), we mainly concentrate on quasars which have a good chance of being influenced by gravitational

microlensing. Our intentions are to detect and analyse characteristic microlensing features in the lightcurves and to determine the time delays between the images of some multiply macrolensed quasars. Microlensing is probably a very rare phenomenon so that most of the results can be used “only” for a study of the intrinsic variability. To distinguish microlensing flares from intrinsic events in a measured lightcurve, high-quality data are required. Most published optical variability data are based on photographic measurements and therefore have a typical relative error of ~ 0.1 mag.

In this paper, being the first one in a series, we exclude from the discussion those quasars of our sample which were known to be optically violent variables (OVVs) prior to our program. We *define* an object as an OVV if it shows variations $\gtrsim 0.5$ mag with gradients $\gtrsim 5 \text{ mag yr}^{-1}$ in the quasar restframe. We here discuss objects with measurements sufficiently spread over a time-span $\gtrsim 2$ yrs. Some interesting properties of these quasars are given in Table 1; Table 4 lists values of some reasonable parameters through which the lightcurve shapes can be quantified. In Fig. 1, we present a selection of our lightcurves; the other curves will be presented in Schramm et al. (1993b, hereafter Paper II). A special discussion of the flaring characteristics of some BL Lac objects and other OVVs will appear in Schramm et al. (1993c, see also Borgeest & Schramm 1992). One of the most interesting OVVs in our sample is 3C 345; our lightcurve together with a detailed discussion of possible variability mechanisms can be found in a separate publication (Schramm et al. 1993a; cf. also Borgeest & Schramm 1992 and Schramm & Borgeest 1992). For another two objects, we already published photometric data separately: GC 0248+430 (cf. Fig. 1), a quasar behind a tidal tail of a merger galaxy system (Borgeest et al. 1991a, hereafter BDHKS), and 0836+710, a high redshift γ -ray source (v. Linde et al. 1993). The lightcurves of the multiply macrolensed quasars in our sample, together with models for the time delays, will be discussed in subsequent papers.

2. Observations and reduction

2.1. Photometric measurements

We use a CCD camera at the Cassegrain focus of the MPIA 1.2m telescope which has been equipped with different chips, in 1988 with an RCA 15μ chip (640×1024 , pixel size $0.315''$)

*Based on observations collected at the German-Spanish Astronomical Centre, Calar Alto, operated by the Max-Planck-Institut für Astronomie (MPIA), Heidelberg, jointly with the Spanish National Commission for Astronomy

and later various, but similar, coated GEC 22μ chips (410×580 , pixel size $0.462''$). We measure the quasar fluxes through standard Johnson broad-band filters (R , V and B) relative to stars included in the frames. The data reduction is carried out automatically, immediately after the observation, on a μ VAX 3200 workstation. Thus interesting features in the lightcurves can be followed with an adequate time resolution, provided that observing time is available at the telescope. Usually, the observations are made in the R -band, where the quantum efficiency of the CCD chips is best; other filters are only used if significant variability is recognized in R . A 0.01 mag accuracy (in relative photometry) in the lightcurve of a ~ 17.5 mag quasar could be reached in this way also for “non-photometric” conditions with a typical exposure time of 500 sec (in R). The error bars ($\pm 1\sigma$) given in Fig. 1 are calculated from $\sigma^2 = \sigma_{\text{ref}}^2 + \sigma_{\text{fit}}^2$ where σ_{ref} is given by the weighted mean of the deviations of the reference star magnitudes from their average values and σ_{fit} is the fit error obtained by fitting a two-dimensional Gaussian function to the quasar profil. σ is therefore an upper limit for the real error as can also be seen by comparing the σ_j in Table 4 with $\bar{\sigma}$ or $\hat{\sigma}$ (cf. Eq. [2]).

2.2. Distribution of observing campaigns

For our program, 15%–30% of the observation time at the MPIA 1.2 m telescope was available during the last years. The program started with regular observations in May 1989. A test period in Sept./Oct. 1988 gave additional data (see e.g. Borgeest et al. 1991b and Schramm & Borgeest 1992). In order to analyse long-term features in the lightcurves, observations are almost equally distributed over the whole year with a typical spacing of two to four weeks between the single campaigns. For a more detailed study of OVVs, nightly photometry is carried out once or twice a year, during campaigns of a few weeks. Until now we obtained more than 7,000 useful photometric data points. Although we tried to observe with regular spacings, a lot of gaps in the lightcurves occurred due to bad weather conditions, closure of the observatory or technical problems.

2.3. Automatic reduction

Since we want to react immediately in the case of a microlensing high-amplification event, a μ Vax 3200-workstation is connected to the MPIA computer which produces the raw frames. The software package “HQM” has been developed in Hamburg; it is much faster than standard image processing software: the photometric reduction of one frame is carried out within 2 to 3 min, during the following exposure. Generally, each quasar is observed twice (e.g. 100 and 500 sec) in the Johnson R filter band for one point in the lightcurve. The shorter exposure is made first and then used for telescope aquisition; hence, there is an angular shift between the exposures. The shorter exposure is very useful for recognizing photometric errors due to cosmic-ray events in one object or chip defects. If a significant difference is found, a third measurement is carried out. In the case of a real brightness change, additional exposures in B and V are made. The HQM-calculations include the following steps: bias subtraction, flatfield correction, object identification and two-dimensional Gaussian fits for the quasar and all stars that can be used as photometric references. For a 500 sec exposure (in R) of a 17.5 mag quasar, this procedure leads to an error in

relative photometry typically between 0.005 and 0.02 mag, depending on seeing, atmospheric transmission, moon light and number of bright reference stars. All these sources of error influence the photon statistics, which has been proved to give the best estimate for the total error (the chip read-out noise can be neglected in most cases). Other sources of error, like cosmic ray events in one of the objects, chip defects or variable reference stars, are rare and the software is designed to recognize and correct for them in most cases. Some data have been taken under very bad conditions, e.g. observation through clouds, seeing $\gtrsim 3''$, full moon near zenith (which causes scattered light on the chip). Even for these cases, the errors in relative photometry ($\lesssim 0.05$ mag) are of the order of (or even better than) those for photographic measurements under good conditions. Such “very bad” data have been included in Fig. 1 only if no better measurements were made during the same night.

2.4. POSS photometry

We used the CCD frames obtained during our program to calibrate the fields around the quasars on R -prints of the Palomar Observatory Sky Survey (POSS). The corresponding Schmidt plates had been obtained during the years 1949 to 1955 so that we were able to determine optical variations for the ~ 40 yr period from ~ 1950 to ~ 1990 . The calibration was carried out by fitting a linear function to the pairs (R_i, x_i) , where R_i are the R magnitudes of the stars from the CCD frames and x_i are the diameters of the black stellar disks on the prints. Each star and quasar diameter has been measured four times, twice in S–N and W–E directions, with the left and right eye, respectively. In Table 4, we list the results of the POSS photometry. The given errors result from the fit errors of linear regression and the internal errors of diameter determination. For some quasars which are marked in Table 4, the errors are rather large since the photometric sequence contains ≤ 4 stars or the star fluxes differ strongly from that of the quasar (for more details see Linnert 1992).

3. Candidates for microlensing

Our sample includes more than 100 objects selected with respect to different criteria and observed with different priority. Tables 1 and 4 list the HQM-quasars which are discussed in this article.

Multiply macrolensed quasars are the only objects for which one can unambiguously separate microlensing from the intrinsic variability. Since the macrolenses are very probably massive galaxies, one may expect relatively high values for the microlensing optical depth and the shear (cf. Kayser et al. 1986, hereafter KRS). Monitoring of these objects is also very important to obtain the time delays between the components from which limits on Hubble’s constant (Borgeest & Refsdal 1984, Falco et al. 1991) and a relative accurate estimate of the lens mass (Borgeest 1986) can be deduced. Unfortunately, most of these objects are not well resolved under average conditions on Calar Alto and the angular scale of the CCD chips which were used does not yield a sufficient sampling, so that the photometric reduction is not straight forward. The work is still in process; we shall discuss our data on multiply lensed quasars in subsequent papers.

Table 1. HQM-quasars discussed in this article. Following the name, the selection technique is indicated: O (optical), R (radio), X (X-ray); V -magnitudes marked with “#” are from the HST snapshot survey (Maoz et al. 1993), otherwise from Véron-Cetty & Véron (1991, hereafter VV); S_6 is the radio flux at 6cm, α the radio spectral index ($S \propto \nu^{-\alpha}$, from VV); S_X the Einstein X-ray flux in $10^{-13} \text{erg s}^{-1} \text{cm}^{-2}$ between 0.3 and 3.5 keV (for Refs see Hewitt & Burbidge 1989); in the following columns, redshifts and restframe equivalent widths (together for both lines) of MgII-absorption systems are given; the last columns list properties of foreground galaxies, θ_a is the approximate radius of a galaxy on a POSS blue print. All references are given in Table 2. Abbreviations: str – strong, med – medium, wk – weak, nd – not detected, x – detected

Object	Name		z_{em}	V	$-M_V$	S_6 [Jy]	α	S_X	z_{abs}	W_r [Å]	Ref	z_{gal}	θ_{gal} ["]	r_{gal} [kpc]	V_{gal}	Ref	
0003+158	PHL 658	ORX	0.450	16.4	26.0	0.34	0.59	32.2	–	–	–	–	–	–	–	–	
0007–000	UM 208	O	2.31	18.7#	27.8	–	–	–	–	–	–	–	25	1.3	18	1	
0013–004	UM 224	O	2.086	18.2#	28.4	–	–	–	0.447	1.1	3	–	–	–	–	–	
0014+813	S5	R	3.380	16.5#	30.8	0.55	0.17	–	1.111	1.5	4	–	–	–	–	–	
									1.113	5.0	–	–	–	–	–	–	
0038–019	PKS	RX	1.690	18.5	27.4	0.28	1.10	3.6	–	–	–	0.017	60	1.4	30	14.4	5
0058+019	PHL 938	O	1.955	17.1#	29.3	–	–	–	0.613	3.2	3	–	–	–	–	–	
0104+318	1E	X	2.027	18.9	27.6	–	–	4.2	nd	–	6	0.111	10	0.9	27	17.5	5
0151+045	PHL 1226	O	0.404	17.9#	24.2	–	–	–	0.160	3.1	7	0.160	6	~1	21	19.1	8
												0.160	11	2.5	40	20.2	
												0.018	55	1.8	29		
0153+744	S5	R	2.338	18.0#	28.5	1.51	0.32	–	–	–	–	–	–	–	–	–	–
0248+430	GC	R	1.316	17.6#	27.6	1.21	–0.38	–	0.394	–	9	0.051	15	0.9	23	15.5	10
0446–208	MC1	R	1.896	17.0	29.3	–	–	–	–	–	–	0.067	13	~1	23		11
0454+039	PKS	R	1.345	16.5	28.8	0.43	–0.12	–	0.860	2.8	12	–	–	–	–	–	–
0731+653	W1	R	3.035	18.2#	29.3	0.04	–	–	0.932	1.4	13	–	–	–	–	–	–
0745+557	1E	X	0.174	17.8	22.2	–	–	8.5	–	–	–	0.004	78	2.4	9	15.3	5
0805+046	4C 05.34	RX	2.877	18.2	29.3	0.31	0.62	x	0.703	1.1	14	–	–	–	–	–	–
									0.960	2.0	–	–	–	–	–	–	–
									1.014	1.6	–	–	–	–	–	–	–
0809+483	3C 196	RX	0.871	17.8	26.2	4.36	0.91	3.0	0.437	4.7	15	–	1.2	–	–	21.9	15
									0.871	–	16	–	1.7	–	–	20.7	–
0903+175	H	O	2.756	18.0#	29.2	–	–	–	–	–	–	0.127	4	–	12	18	19
0955+326	Ton 469	RX	0.533	15.8	27.1	0.85	0.28	x	0.513	0.2	20	0.005	114	2.0	16	–	11
1011+250	Ton 490	ORX	1.631	16.6	29.3	0.61	–0.26	x	0.258	wk	21	–	–	–	–	–	–
1109+357	1E	X	0.909	18.1	26.0	–	–	3.8	–	–	–	0.027	26	0.7	21	14.5	5
1150+497	LB 2136	OR	0.334	17.1	24.6	1.12	0.57	–	–	–	–	0.290	7	–	38	20	22
1209+107	KP 9	O	2.191	18.1#	28.6	–	–	–	0.630	5.0	23	0.63?	1.4	–	11	22.3	24
									0.393	1.6	24	0.393	7	–	45	21.2	–
1219+755	Mkn 205	OX	0.072	15.2	22.9	0.00	–	170.0	–	–	–	0.006	42	0.5	7	–	5
1222+228	Ton 1530	OX	2.051	16.6	29.9	0.01	–	2.1	0.669	0.6	3	–	–	–	–	–	–
1332+552	4C 55.27	R	1.249	16.0	29.1	0.13	0.67	–	0.374	str	25	0.374	5	–	32	20.7	25
1421+330	Mkn 679	O	1.904	16.7	29.6	–	–	–	0.456	0.4	17	–	–	–	–	–	–
1435+638	S4	R	2.060	15.0	31.5	1.24	0.21	–	nd	–	3	–	–	–	–	–	–
1520+413	SP 43	O	3.1	18.7#	28.6	–	–	–	–	–	–	–	–	–	–	–	–
1522+101	PG	O	1.321	16.2#	29.1	0.00	–	–	–	–	–	0.0	–	0	–	–	26
1604+290	KP 63	OR	1.97	17.0	29.4	0.00	1.49	–	–	–	–	7.5	–	–	19.5	–	1
1630+377	PG	O	1.471	16.1	29.5	0.00	–	–	–	–	–	9.5	–	–	21	–	1
									–	–	–	15	–	–	20	–	–
1633+267	KP 83	O	1.84	17.0	29.2	–	–	–	–	–	–	39	–	–	18	–	1
1634+706	PG	OX	1.334	14.9	30.5	0.00	–	8.0	0.993	1.0	2	–	–	–	–	–	–
									1.046	0.1	–	–	–	–	–	–	–
1640+396	1E	XR	0.540	18.3	24.6	0.03	–	6.6	–	–	–	0.034	200	4.7	200	15.2	5
1700+642	HS	O	2.72	16.1	31.1	–	–	–	–	–	–	0.086	11	–	24	18.8	27
									–	–	–	0.19	18	–	75	–	–
1701+610		X	0.164	17.0	22.9	–	–	x	–	–	–	0.052	29	~4	40	–	28
									–	–	–	0.052	38	~5	53	–	–
1704+608	3C 351	RX	0.371	15.3	26.6	1.21	0.84	10.4	0.163	–	29	–	–	–	–	–	–
									0.222	–	–	–	–	–	–	–	–
1715+535	PG	O	1.929	16.5	29.8	0.00	–	–	0.367	0.6	3	–	–	–	–	–	–
1718+481	PG	O	1.084	14.7	29.9	0.14	–	–	0.713	–	2	–	–	–	–	–	–
1821+643	E	X	0.297	14.2	27.1	–	–	x	–	–	–	–	–	–	–	–	–
1857+566	4C 56.28	R	1.595	17.3	28.5	0.23	1.44	–	0.715	1.3	30	–	3	–	–	–	18
									1.106	0.6	–	–	–	–	–	–	–
									1.235	1.5	–	–	–	–	–	–	–
2126–158	PKS	RX	3.266	17.0#	30.3	1.24	–0.09	26.0	2.022	1.0	31	–	–	–	–	–	–
2134+004	PHL 61	ORX	1.936	17.1#	29.2	11.49	–0.67	x	–	–	–	–	–	–	–	–	–
2215–037	X	X	0.241	17.2	23.7	–	–	x	–	–	–	0.061	14	~2	23	–	32
2251+244	4C 24.61	R	2.328	18.5#	28.0	0.79	0.93	–	1.090	0.9	30	–	0.8	–	–	–	18
2308+098	4C 09.72	R	0.432	16.0	26.3	0.25	0.59	–	–	–	–	0.173	9	–	35	–	22
2354+144	PKS	R	1.813	18.2	27.9	0.37	0.81	–	1.576	1.6	30	–	4.4	–	–	–	18

Table 2. References for Table 1

1. This work
2. Bechtold et al. 1984
3. Sargent et. al. 1988a
4. Kühr et al. 1984
5. Stocke et al. 1987
6. Blades 1988
7. Bergeron et al. 1988
8. Bergeron 1988
9. Sargent & Steidel 1990
10. Borgeest et al. 1991a
11. Blades et al. 1981
12. Burbidge et al. 1977
13. Sargent et. al. 1989
14. Chen et. al. 1981
15. Boissé & Boulade 1990
16. Foltz et al. 1988
17. Foltz et al. 1986
18. Crampton et al. 1989
19. Djorgovski & McCarthy 1985
20. Boksenberg & Sargent 1978
21. Carswell et al. 1976
22. Stockton 1978
23. Cristiani 1987
24. Arnaud et al. 1988
25. Miller et al. 1987
26. Magain et al. 1990
27. Reimers et al. 1989
28. Hutchings et al. 1986
29. Jenkins et al. 1987
30. Barthel et al. 1990
31. Usher 1978
32. Heckman et al. 1984

3.1. Quasar-galaxy associations

We have selected from the literature many quasars with closely associated foreground galaxies. In our opinion, only for those foreground galaxies which lie not too far (i.e. $\lesssim 50$ kpc)¹ from the line of sight to a quasar, a relatively high optical depth for microlensing can be expected. Also interesting are those cases where a quasar shines through a foreground galaxy within their optical isophotes (cf. column 15 of Table 1). We have denoted these objects by *G1*; other quasars with associated foreground galaxies are denoted by *G2*, see Table 3.

Stocke et al. (1987, hereafter SSMG) searched for bright ($m_V \lesssim 18$) galaxies near the members of a sample of more than 200 X-ray selected AGN on POSS plates. They found that the redshift distribution of those 10 AGN lying within 3 optical radii of foreground galaxies have a much higher percentage of high redshift objects than the total sample. They interpret this result in terms of an amplification bias due to microlensing. The total sample includes a subsample of 56 AGN complete in X-ray flux (Maccacaro et al. 1984) which was observed by Rix & Hogan (1988) by CCD imaging (search limit for galaxies $m_R \simeq 20.5$); they found 5 additional AGN near

galaxies, but could not verify the result of SSMG. The largest problem is the small number of objects near foreground galaxies in both studies, therefore statistically significant results are difficult to obtain out of their redshift distributions. In our opinion it is, however, very interesting that the two objects with the highest X-ray luminosity ($L_X \gtrsim 10^{28}$ ergs Hz⁻¹ s⁻¹) in the complete sample have a foreground galaxy, compared to only 6 of the 54 less luminous ones. Both objects, 1E 0038–019 and 1E 0104+318, are highly luminous in the optical, too; and the first one is known to be radio loud. These might be hints on a triple or double amplification bias, respectively (cf. Borgeest et al. 1991c).

We have included 6 objects of the SSMG sample in the HQM program (0038–019, 0104+318, 0745+557, 1109+357, 1219+755, 1640+396) to search for indications of microlensing variability.

3.2. Narrow-absorption-line quasars

From a uniform spectroscopic survey of 55 high redshift QSOs, Sargent, Boksenberg & Steidel (1988a, hereafter SBS) obtained 40 Mg II-absorption systems. The large scale distribution of the redshifts is random and therefore consistent with the intervening hypothesis for the origin of the lines. Very probably, most MgII-absorption systems arise from intervening galaxies. This assumption is confirmed by the work of Bergeron (1988) who found an image of a galaxy $< 10''$ from the quasar in 10 out of 14 cases of MgII absorption. All galaxies agree in redshift with the absorption systems. The large average number of about 0.7 Mg II-absorption systems per quasar found by SBS and the result of Bergeron indicate that in most cases the absorption occurs far away from the centre of the foreground galaxy, in its extended halo where one would expect a low density of stars. In our opinion, only MgII systems having large equivalent widths make it more probable that the quasar light passes regions of higher star density. We have included in our sample some quasars with MgII-absorption lines of rest frame equivalent widths $W_r > 1\text{\AA}$ (together for both lines of the doublet); these objects are denoted *A1*.

3.3. Highly luminous quasars

There is increasing observational evidence for a so-called amplification bias (AB, sometimes “magnification bias” is also used) by gravitational lensing; i.e. an enhancement of foreground galaxies around quasars out of flux (or luminosity) limited samples. Many authors discuss the AB as a result of microlensing (for Refs. see Borgeest et al. 1991c). We have included in our sample a number of highly luminous quasars (*HLS*, $M_V < -29.0$). Probably, the *HLS* are subject to a strong AB. If microlensing indeed contributes significantly to the AB in our sample of highly luminous quasars, strong microlensing variability must be found in the lightcurves of these quasars.

4. Discussion of the lightcurves

4.1. Literature data

Extensive monitoring programs which include low amplitude variability quasars have been carried out by several investigators:

- At the Rosemary Hill Observatory more than 200, mostly radio-selected quasars were monitored since 1968, however

¹We use $H_0 = 50$ km s⁻¹ Mpc⁻¹, $q_0 = 0$ throughout this paper.

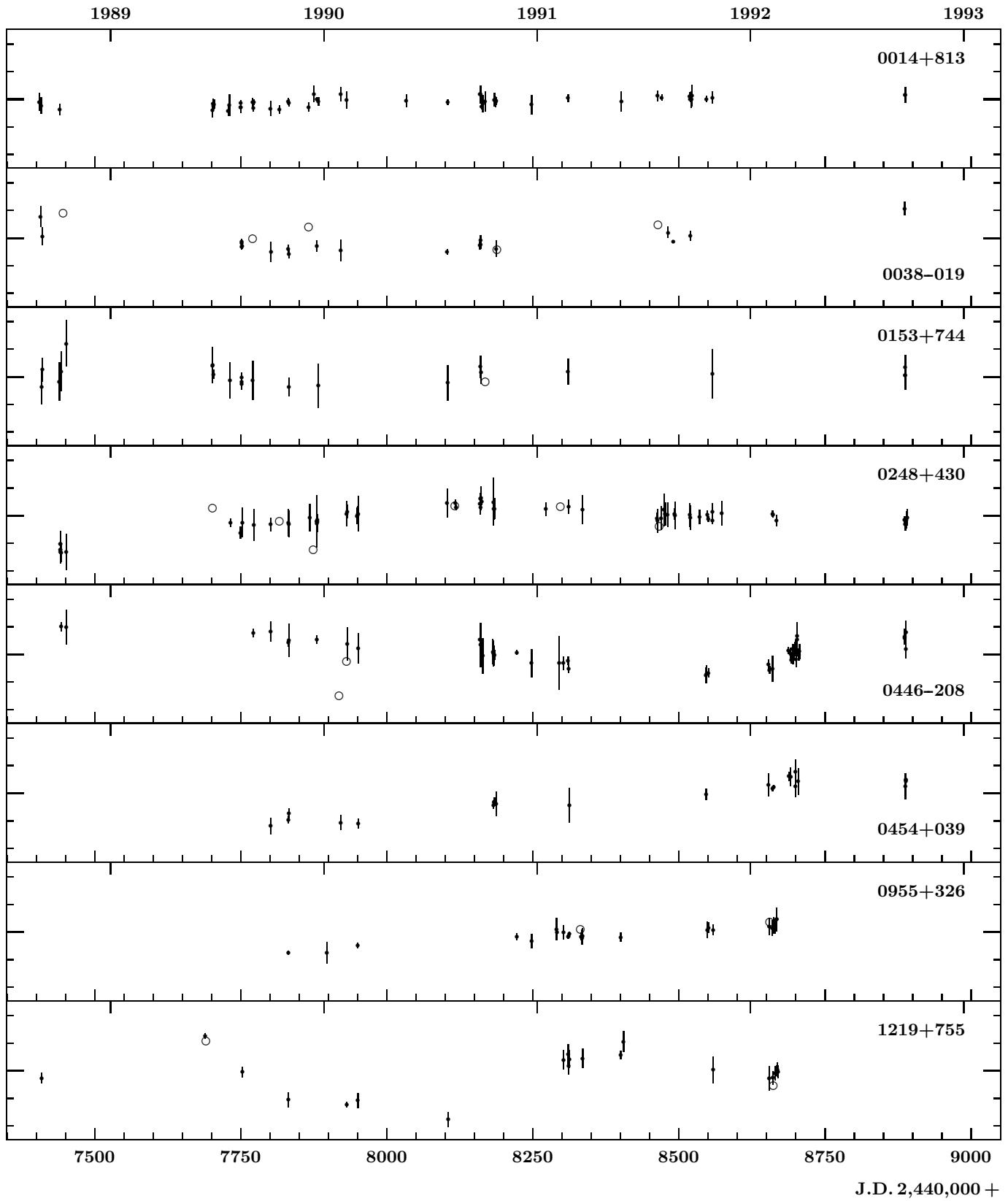


Fig. 1. HQM lightcurves in the R -band. Dashes on the vertical axes represent 0.1 mag steps. Plotted are variations $\Delta R = R_0 - R$; the reference magnitude R_0 is indicated by thick dashes. Measurements obtained under very bad atmospheric conditions or those with only one reference star are shown by open circles; reliable error bars can in these cases not be given

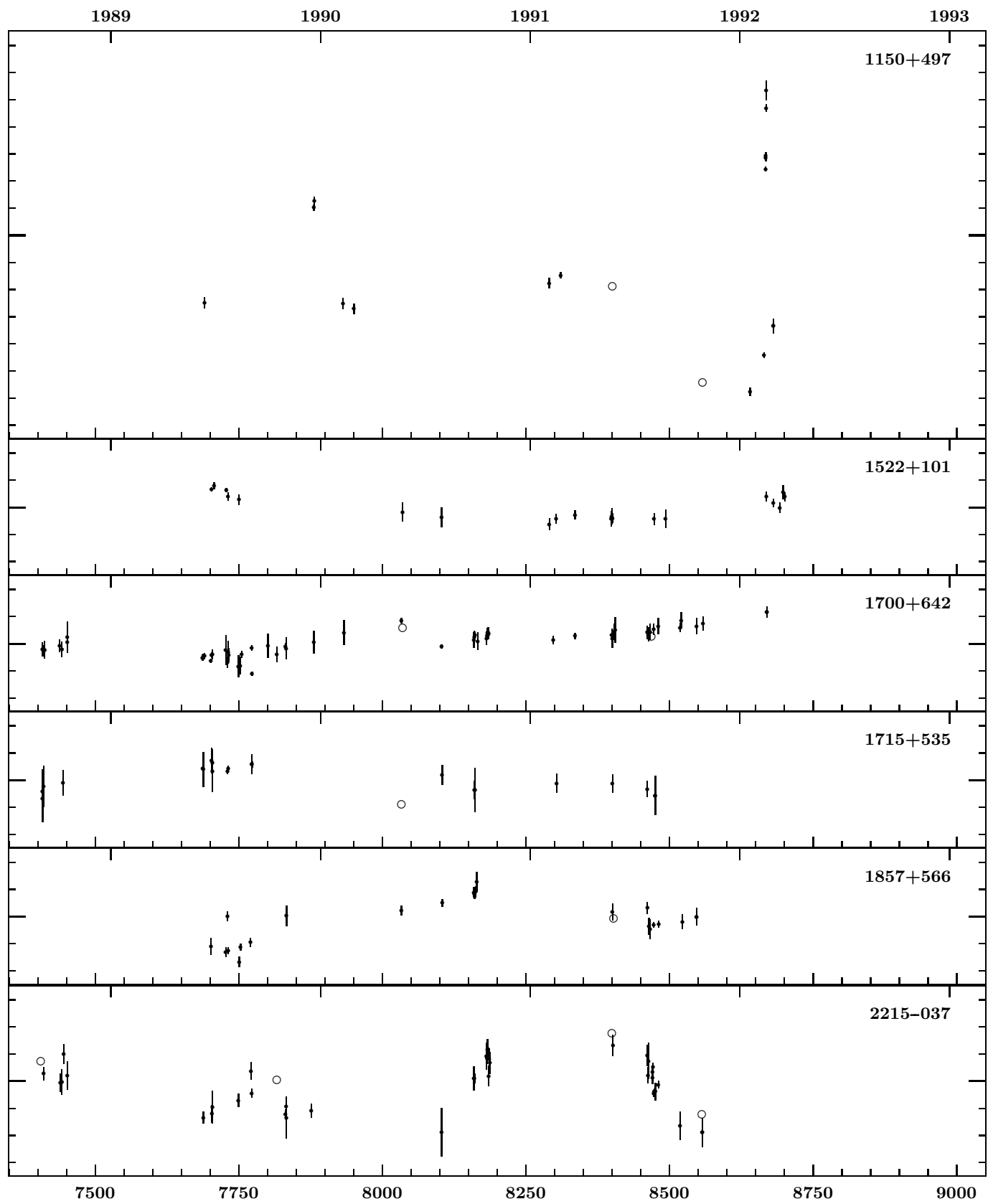


Fig. 1. (continued)

J.D. 2,440,000 +

Table 3. *A priori* selection criteria for the sample

Class	Definition
<i>A1</i>	MgII absorption quasars with $W_r \gtrsim 1 \text{ \AA}$, together for both lines of the doublet
<i>G1</i>	(i) Objects having the image of an associated foreground galaxy with $z_{\text{gal}} \gtrsim 0.05$ closer than 50 kpc to the line of sight, or (ii) objects located within 1 optical radii, θ_a (see Table 1), of a foreground galaxy
<i>G2</i>	(i) Objects having the image of an associated foreground galaxy with $z_{\text{gal}} \gtrsim 0.05$ between 50 and 100 kpc from the line of sight, or (ii) objects located between 1 and 2 optical radii from a foreground galaxy
<i>HL</i>	Optically highly luminous quasars, $M_V \leq -28.0$ (for known variable objects, the maximum flux values found in the literature have been taken)
<i>Ra</i>	Quasars from large-area radio surveys

not all objects over the total period (Pica et al. 1980, hereafter PPSL; Pica & Smith 1983, hereafter PS83; Smith et al. 1993, hereafter SNLC, and Refs. therein).

- Lloyd (1984, hereafter L84) reports on lightcurves of 36 radio sources from the Herstmonceux Optical Monitoring program for the period 1966-1980 (see also Tritton & Selmes 1971, hereafter TS71; Selmes et al. 1975, hereafter STW).
- Another program has been carried out at the Asagio Observatory (e.g. Barbieri et al. 1979, hereafter BRZ) over the period 1967 to 1977.
- Monitoring data obtained until 1973 are reviewed and critically discussed by Grandi & Tift (1974, hereafter GT74).
- Moore & Stockman (1984, hereafter MS84) have collected a catalog of the observational properties of 239 quasars, including variability data.
- Lightcurves of many bright quasars have been obtained from the Harvard historical plate collection (e.g. Angione 1973, hereafter A73) spanning periods of up to 100 years.
- Netzer & Sheffer (1983, hereafter NS83) compared the 1981 and ~ 1950 POSS magnitudes of 64 optically selected UM quasars. They found that 39% of the quasars have varied by more than 0.45 mag.

More recent publications on optical variability of quasars generally deal with violent variable sources.

4.2. HQM lightcurves

In this section, we compare the lightcurves plotted in this paper with those of previous work. The other HQM lightcurves are discussed in Paper II.

S5 0014+813. There are no variability data in the literature. The only feature in the well sampled HQM lightcurve is a very weak linear brightening of $0.014 \pm 0.002 \text{ mag yr}^{-1}$. To our knowledge, it has up to now not been possible to determine a long-term trend in an optical quasar lightcurve with this accuracy.

PKS 0038–019. There are no variability data in the literature. Our HQM data are well described by a second order polynomial.

S5 0153+744. There are no variability data in the literature. The HQM lightcurve is consistent with a constant flux. A hint on moderate variability comes only from the POSS photometry. On our best frames, an enhancement of faint galaxies is obvious in the vicinity of the quasar.

GC 0248+430. The only optical variability data in the literature are from our HQM program (see BDHKS). Besides a steady increase until the beginning of 1990, we reported the possible detection of short-term variability. A reevaluation of the data has however shown that there is probably no short-term activity: The photometric points which deviate from the main trend were all obtained during poor atmospheric conditions. The more recent data show that the quasar is fading again. BDHKS have collected literature data on radio measurements showing that the object is much more active in the radio wavelength range.

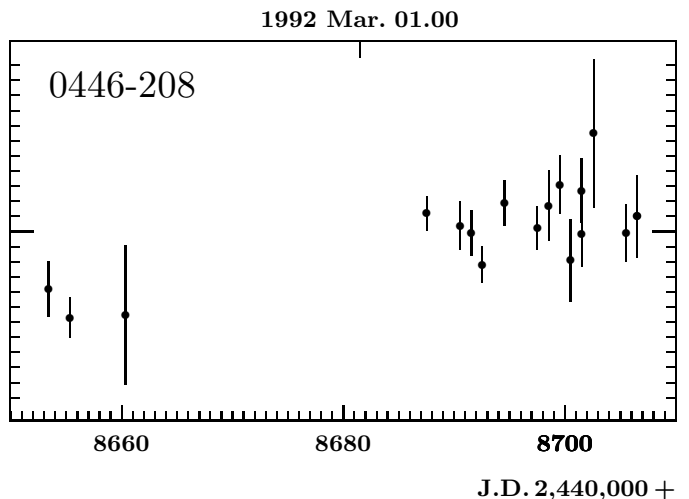


Fig. 2. Enlarged presentation of the winter '92 lightcurve of the quasar MC1 (0446-208) in Johnson-*R*. Here, dashes on the vertical axes indicate 0.01 mag-steps. The only significant feature is an overall brightening

0446–208 (MC 1). There are no variability data in the literature. The HQM lightcurve is sufficiently sampled to show the structure of a weak variability which is well described by a third order polynomial. The winter 1992 lightcurve is plotted with higher resolution in Fig. 2.

PKS 0454+039. There are no variability data in the literature. The HQM data show that the object is brightening by $\sim 0.06 \text{ mag yr}^{-1}$. Our POSS photometry yields also some evidence for moderate variability.

Ton 469 (0955+326). L84 recorded a smooth lightcurve between 1967 and 1979, showing a broad minimum and a total amplitude $\Delta B \simeq 0.5 \text{ mag}$. Xie et al. (1988) searched for variations during one single night, Jan. 1, 1987, with a negative result. In the UV, however, a change in flux by a factor of 2 was recorded during one day (Bruhweiler et al. 1986). The historical lightcurve measured by A73 has large scatter with $\sigma_0 = 0.27 \text{ mag}$. The only significant feature in the HQM lightcurve is a linear brightening by $\sim 0.04 \text{ mag yr}^{-1}$.

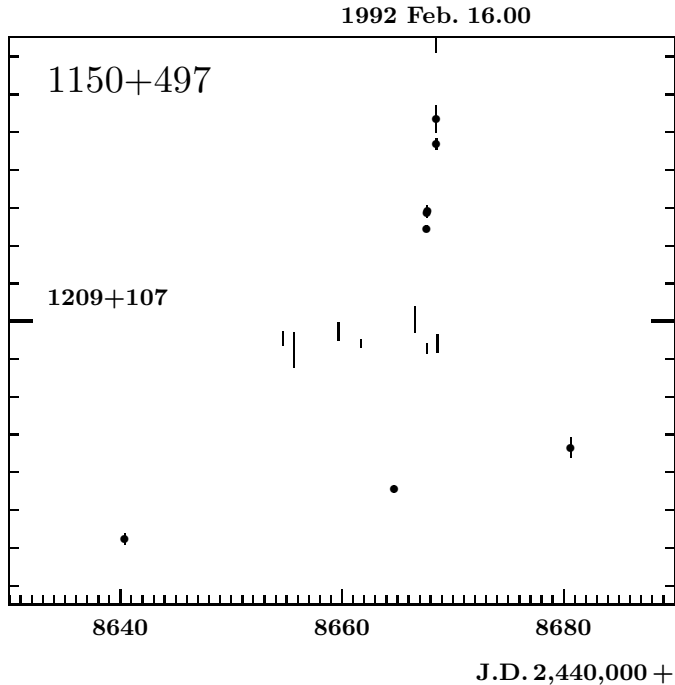


Fig. 3. R -lightcurve of LB 2126 (1150+497) in winter '92. For comparison, data for Q 1209+107 (error bars only) are also shown; the latter object was observed between the exposures of LB 2126 on Feb. 15 (40 min difference), it shows no indication of variability

LB 2136 (1150+497). BRZ found, between 1967 and 1976, a total range of variability $\Delta B \simeq 1.4$ mag. A 0.25 mag fading was recorded by TS71 between 1967 and 1968. Radio variability was detected by Moore et al. (1981). Besides 0836+710 (see v. Linde et al. 1993) LB 2126 is the only object for which violent variability was detected during the HQM program *and* which was not known to be an OVV before. A rapid flare was recorded on Feb. 15/16, 1992 (Fig. 3). Interestingly, a flare in 0836+710 occurred nearly simultaneously (Feb. 16/17, 1992). One may therefore suspect that a systematic error had “produced” the flares. We looked very carefully for possible sources of such an error, without any result. In Fig. 3, we have also plotted the lightcurve for 1209+107. One measurement for this object was made between two exposures of LB 2126 on Feb. 15; there is absolutely no indication for an error above our estimate. With the knowledge that flares are occurring in the lightcurve of LB 2126, one may assume in the data of BRZ another flare, in early summer 1972. The radio spectral index of LB 2126 in the catalogue of VV is $\alpha = 0.57$, close to the value which separates steep spectra from flat ones. In addition, the object is a core-jet VLBI source. One may therefore assume that LB 2126 belongs to the blazar class. This hypothesis can only be tested by further observations.

Mkn 205 (1219+755). Zamorani et al. (1984) detected 20% X-ray variability on a timescale of about one day. Our optical data show significant variations, too, however on a longer timescale. The lightcurve can be fitted by a fourth order polynomial or a sine function of a period not much longer than the total timespan of observations. POSS photometry also indicates variability.

PG 1522+101. There are no variability data in the literature. The HQM data clearly indicate variations, well fitted by a sec-

ond order polynomial. Very close to the quasar lies a probably interacting pair of galaxies which we detected in May 1989 on a deep frame taken with the 2.2m telescope; after subtraction of the pointspread function on an exposure obtained at ESO, Magain et al. (1990) found a third galaxy just on the top of the quasar image.

HS 1700+642. There are no variability data in the literature for this very luminous object. Due to the good sampling some details in the weak variability are seen in the HQM lightcurve.

PG 1715+535. There are no variability data in the literature. Our lightcurve is consistent with a constant flux, although the 1989/90 data seem to indicate a slight brightening. The photometric errors are relatively large due to an unresolved object 6'' from the quasar. Due to a “quick-look” spectrum obtained at the MPIA 3.5m telescope, kindly provided by H. Hagen, this object is identified as a star .

4C 56.28 (1857+566). There are no variability data in the literature. The main trend in the HQM lightcurve is well fitted by a second order polynomial. A few isolated points show significant deviations from the best fit; it is not clear whether this is a real effect. POSS photometry indicates variations on a very long time scale, too.

2215-037. Pica et al. (1987) recorded a long-term steady increase of $\Delta B \simeq 1$ mag over 17 years and also found some evidence for short-term variability. The HQM data also indicate short-term variations on a timescale comparable with the time lags between the observing campaigns.

5. Statistical results

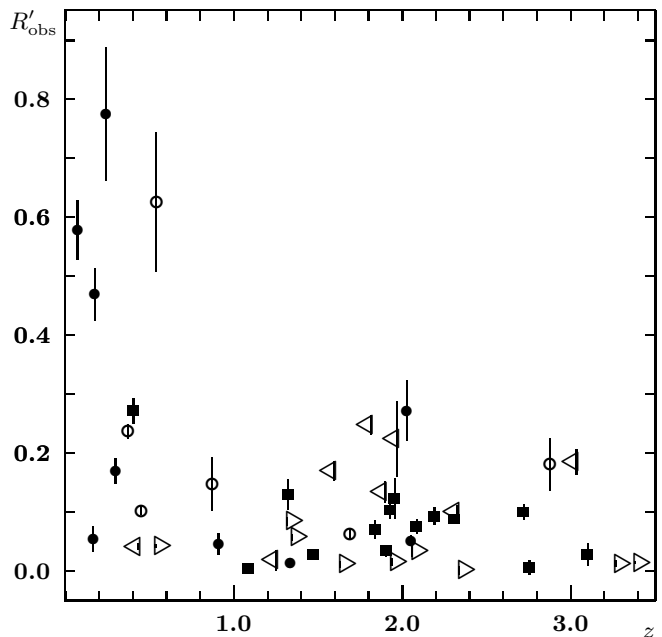


Fig. 4. Maximum gradients R'_{obs} in the observer's restframe plotted versus z . *Filled squares:* radio quiet, X-ray quiet; *•:* radio quiet, X-ray loud; *◦:* radio loud, X-ray loud; *◁:* steep-spectrum radio quasars; *▷:* flat-spectrum radio quasars

As noted above, the sub-sample of quasars discussed in this paper results from excluding those objects which were known to be of OVV type. In Table 4, we list some reasonable parameters which describe the lightcurves quantitatively. We give the

Table 4. Results of HQM and POSS photometry. In column 2, those objects are marked which were previously known to be variable; in column 3, we give the *a priori* selection criteria through which the corresponding object entered our sample (cf. Table 3). For definitions of the quantities listed in the following columns, see text

Object	Var	Class	n'	n	Δt [yrs]	\hat{n}	$\bar{\sigma}$ [mag]	$\tilde{\sigma}$	σ_0	σ_1	σ_2 [mag]	σ_3	σ_4	σ_5	R'_{obs} [mag yr ⁻¹]	ΔR_{40} [mag]
0003+158	×	<i>Ra</i>	17	16	4.04	4.6	.025	.026	.077	.066	.064	.014	—	—	-0.102±.006	+0.72±.12
0007-000	×	<i>G2</i>	5	4	4.05	3.5	.013	.014	.146	.007	—	—	—	—	-0.088±.002	-0.01±.30 ^{*,\dagger}
0013-004	×	<i>A1</i>	10	10	3.10	4.4	.028	.031	.054	.019	.019	.016	—	—	-0.075±.012	+0.09±.23 \dagger
0014+843		<i>A1</i>	63	54	4.06	10.8	.022	.023	.020	.015	.015	.015	.014	.014	+0.014±.002	-0.08±.21
0038-019		<i>G2</i>	30	23	4.05	7.3	.025	.027	.045	.040	.017	—	—	—	+0.063±.008	+0.00±.31
0058+019	×	<i>A1</i>	15	14	4.04	5.6	.022	.024	.053	.048	.033	.033	.017	—	+0.123±.034	+0.04±.41 [*]
0104+318	×	<i>G1</i>	12	8	3.25	5.3	.063	.072	.091	.087	—	—	—	—	-0.272±.050	-0.57±.23 \dagger
0151+045	×	<i>G1</i>	39	25	4.05	6.8	.020	.022	.138	.096	.094	.045	.031	—	+0.227±.021	+0.35±.36
0153+744		<i>HL</i>	24	24	4.05	8.0	.052	.056	.035	.035	.033	.033	.033	.029	-0.001±.006	-0.65±.20
0248+430		<i>G1</i>	160	79	3.97	13.4	.027	.029	.046	.043	.027	.025	.023	.023	+0.084±.006	-0.10±.18
0446-208		<i>G1</i>	77	56	3.96	9.2	.026	.028	.042	.040	.030	.026	.026	.023	+0.134±.017	+0.23±.20
0454+039		<i>A1</i>	36	31	2.98	7.6	.027	.029	.060	.027	.026	.026	.026	.022	+0.057±.005	-0.23±.10
0731+653		<i>A1</i>	26	16	2.29	5.0	.024	.026	.088	.060	.035	.034	—	—	+0.185±.021	-0.37±.18
0745+557		<i>G2</i>	15	13	2.27	4.3	.034	.040	.105	.045	.038	—	—	—	-0.469±.044	-0.12±.26
0805+046	×	<i>A1</i>	7	6	2.39	3.8	.042	.046	.103	.057	—	—	—	—	+0.181±.044	-0.09±.23
0809+483	×	<i>G1</i>	23	20	2.29	5.2	.046	.054	.079	.036	.019	.018	.017	—	+0.147±.013	-0.32±.44 [*]
0903+175		<i>G1</i>	28	15	2.39	5.4	.040	.045	.034	.033	.028	.023	.023	—	-0.006±.011	+0.08±.20
0955+326	×	<i>G2</i>	45	42	2.29	6.8	.018	.020	.028	.013	.013	.013	.013	.013	+0.042±.003	-0.07±.40 [*]
1011+250	×	<i>HL</i>	19	18	2.35	5.6	.023	.026	.022	.020	.020	.019	.014	—	+0.011±.005	-0.10±.51 ^{*,\dagger}
1109+357		<i>G1</i>	14	6	2.16	4.1	.067	.079	.049	.031	—	—	—	—	-0.046±.018	-0.10±.32 \dagger
1150+497	×	<i>G2</i>	19	19	2.71	6.0	.022	.028	OVV						+91±11	+0.17±.23
1209+107		<i>G1</i>	18	10	2.02	4.3	.028	.032	.081	.022	—	—	—	—	-0.093±.014	+0.01±.22
1219+755		<i>G1</i>	46	33	3.45	9.4	.033	.036	.071	.071	.071	.065	.035	.023	-0.579±.050	-0.76±.30
1222+228		<i>HL</i>	12	10	1.92	4.6	.019	.020	.019	.017	.009	—	—	—	-0.052±.008	+0.28±.24
1332+552	×	<i>G2</i>	9	6	1.77	4.3	.046	.058	.023	.020	.018	—	—	—	-0.018±.017	-0.74±.15
1421+330		<i>HL</i>	11	11	2.68	4.8	.009	.009	.023	.021	.011	—	—	—	-0.034±.009	+0.44±.46 [*]
1435+638		<i>HL</i>	14	13	3.45	3.9	.016	.019	.053	.018	.013	—	—	—	+0.038±.004	+1.57±.20 \dagger
1520+413		<i>HL</i>	13	11	2.20	4.5	.033	.034	.054	.049	.044	—	—	—	-0.028±.019	-0.17±.45
1522+101		<i>G1</i>	29	27	2.73	7.1	.021	.022	.047	.046	.018	.018	.017	.017	+0.130±.026	+0.17±.39
1604+290		<i>HL</i>	27	16	2.68	5.8	.041	.048	.102	.071	.042	.042	—	—	-0.223±.063	-0.29±.29
1630+377		<i>HL</i>	24	23	2.38	6.6	.021	.023	.030	.020	.019	.018	.018	—	+0.028±.005	+0.03±.22
1633+267		<i>HL</i>	13	11	2.16	4.9	.039	.046	.065	.035	.022	—	—	—	-0.070±.015	-0.39±.15
1634+706		<i>A1</i>	17	17	2.16	6.1	.013	.014	.022	.019	.019	.019	.018	—	+0.014±.006	+0.35±.20
1640+396		<i>Ra</i>	37	22	2.61	5.4	.034	.041	.126	.126	.122	.071	—	—	+0.626±.118	+0.02±.23
1700+642		<i>G1</i>	79	42	3.45	14.5	.022	.024	.049	.030	.027	.026	.023	.022	+0.100±.013	+0.09±.17
1701+610		<i>G2</i>	22	12	2.38	4.4	.043	.046	.084	.066	.064	—	—	—	-0.054±.021	-0.91±.37 [*]
1704+608	×	<i>Ra</i>	51	45	2.18	6.2	.018	.019	.071	.026	.025	.012	—	—	+0.237±.012	—
1715+535		<i>HL</i>	38	11	2.92	9.1	.030	.034	.038	.029	.023	.015	.015	—	+0.103±.013	-0.13±.24
1718+481		<i>HL</i>	21	21	2.94	4.6	.018	.019	.012	.011	.009	—	—	—	-0.004±.003	+0.01±.25
1821+643			15	14	2.09	5.4	.014	.015	.032	.026	.010	.005	—	—	-0.169±.021	-0.70±.28
1857+566		<i>A1</i>	36	31	2.32	7.2	.025	.028	.081	.074	.038	.037	.032	.031	+0.170±.016	+0.70±.19
2126-158		<i>A1</i>	14	11	2.92	4.6	.022	.024	.021	.016	.016	—	—	—	+0.012±.005	-0.20±.23
2134+004	×	<i>HL</i>	21	18	2.93	7.0	.019	.020	.032	.027	.027	.027	.024	.021	-0.015±.006	-0.08±.34
2215-037		<i>G1</i>	67	43	3.15	8.8	.033	.037	.089	.088	.088	.064	.057	.057	-0.775±.113	+0.21±.25
2251+244		<i>G1</i>	44	21	1.97	6.3	.032	.042	.050	.026	.017	—	—	—	-0.100±.010	-0.22±.37
2308+098		<i>G2</i>	11	10	2.84	4.0	.014	.016	.056	.019	.016	—	—	—	+0.041±.005	+0.30±.24
2354+144	×	<i>G1</i>	17	13	2.28	5.2	.028	.033	.105	.099	.028	.027	—	—	-0.248±.016	+1.08±.32 \dagger

* There are only less than five stars in the CCD frames which are useful for POSS photometry

\dagger All useful stars are brighter than the quasar

total number n' of data points and the total timespan Δt of observation; n is the number of points used for further analyses, data with the largest errors have been dropped. The number \hat{n} describes the sampling:

$$\hat{n} = \frac{(t_n - t_1)^2}{\sum_{i=1}^{n-1} (t_{i+1} - t_i)^2} + 1 \quad (1)$$

For equally distributed measurements we have $\hat{n} = n$; whereas $\hat{n} = 2$ means that measurements were only carried

out at t_1 or t_n . The photometric errors in a lightcurve are described by two parameters

$$\bar{\sigma} = \frac{1}{n} \sum_{i=1}^n \sigma_i \quad \text{and} \quad \tilde{\sigma}^2 = \frac{1}{n} \sum_{i=1}^n \sigma_i^2, \quad (2)$$

where σ_i is the error of a single measurement. The standard deviation of the n data points is denoted σ_0 . We have calculated polynomial fits of order $j < \hat{n} - 1$ for each lightcurve. The standard deviation of the points from such fits is then denoted

σ_j . Obviously σ_j decreases with increasing j . A lightcurve is well described by a polynomial fit of order j when $\sigma_j \simeq \bar{\sigma}$. R'_{obs} is the *maximum* observed gradient in each lightcurve; the value is a conservative one, well determined by several data. ΔR_{40} is the result of our POSS photometry.

The maximum lightcurve gradients R'_{obs} are plotted versus redshift z in Fig. 4. It is obvious that there is an anti-correlation. When transforming the variations into the quasar restframes

$$R'_{\text{qso}} = (1+z)R'_{\text{obs}}, \quad (3)$$

and plotting R'_{qso} versus z , cf. Fig. 5, there seems to be no correlation any more. Thus we have no indication for a redshift dependence of the intrinsic variability behaviour. It is also interesting that there is no dependence on the absolute luminosity, M_V (not plotted here).

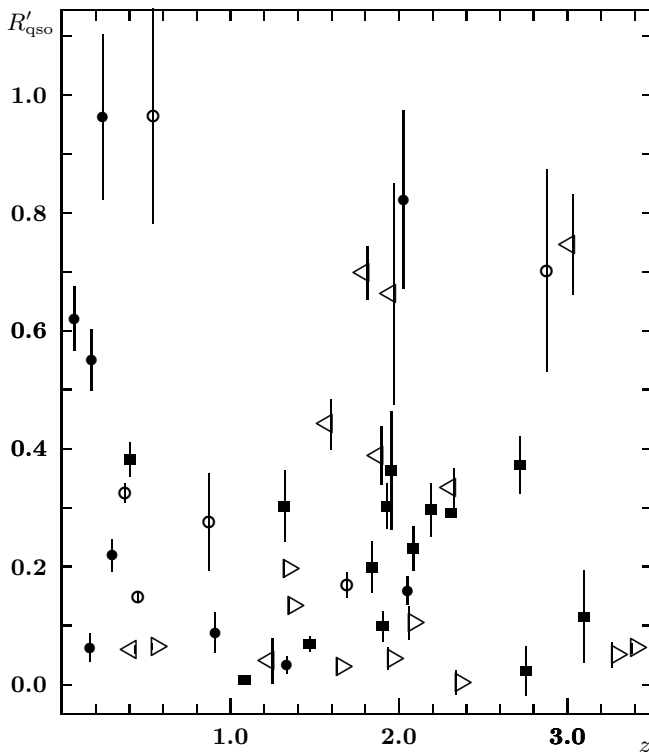


Fig. 5. Maximum gradients R'_{qso} in the quasars' restframes plotted versus z . Same symbols as in the previous figure

5.1. Correlation with radio properties

The intrinsic lightcurve gradients seem, however, to be correlated with the radio and X-ray properties of the quasars. None of the radio *and* X-ray quiet objects, marked by filled squares in Fig. 5, has an intrinsic lightcurve gradient above 0.4 mag yr^{-1} . Even less variable are the flat-spectrum radio quasars, marked in Fig. 5 by triangles pointing to the right; none has an intrinsic lightcurve gradient above 0.2 mag yr^{-1} . In Table 5, we list the average intrinsic variation indices for three different sub-samples.

Bregman (1990) argues that all quasars can be divided into two broad classes: radio quiet objects whose continuum emission is dominated by thermal emission and blazars showing

Table 5. Average intrinsic variation indices $\langle R'_{\text{qso}} \rangle$ for different quasar sub-samples

Sub-sample	N	$\langle R'_{\text{qso}} \rangle$
Radio quiet, X-ray quiet	14	0.218 ± 0.037
Radio-Flat	9	0.076 ± 0.021
Others	23	0.412 ± 0.066

predominately non-thermal emission. Note that many objects may represent mixed types. Angel and Stockman (1980) defined blazars as objects showing flat radio spectra, violent radio and optical variability, high and strongly variable optical polarization and steep non-thermal optical continua. All objects of our total HQM sample which show violent optical variability are radio loud. Most of them have a flat radio spectrum and fulfill also other blazar criteria if one has looked for them; the class of OVVs will be discussed in more detail in a subsequent paper. None of the radio-quiet objects in our sample show violent optical variability. Following Bregman, the optical emission of these objects is thermal radiation from an accretion disk. We conclude from our data that *the thermal radiation from an accretion disk is only weakly variable*. X-ray loud and/or steep-spectrum radio quasars are a bit more strongly variable. We therefore assume an additional radiation mechanism in the optical. Possibly, these objects represent certain mixed types as noted above.

Our lightcurves clearly show that not all flat-spectrum radio quasars are blazars. The flat-spectrum sources discussed in this paper are even less variable in the optical than radio quiet quasars. One should keep in mind that our observations only cover a relatively short time-span; however, L84 already noted that there is “a population of well-observed compact flat-spectrum radio sources which undergo only modest variations over periods of $\sim 80 \text{ yr}$ ”. For some objects it is known that they are more strongly variable in the radio than in the optical (e.g. GC 0248+430). If the variable radio emission originates in synchrotron radiation from a jet, the jet seems to be quiet in the optical for these objects. The optical spectrum should therefore be similar to that of radio quiet objects.

We can only speculate about the origin of the very low degree of optical variability for this class of flat-spectrum radio sources. If one believes that the radio properties indicate a jet roughly orientated towards the observer, the accretion disk will be viewed face on. This orientation effect may be responsible for the extremely low optical variability.

5.2. Microlensing

Chang & Refsdal (1979) were the first to show theoretically that stars in a foreground galaxy may induce significant non-intrinsic variability in the lightcurve of a quasar due to gravitational microlensing. Gott (1981) proposed that it should be possible to detect low-mass stars in galaxy haloes by this effect. Chang & Refsdal (1984), Paczynski (1986) and KRS developed a set of parameters to describe the microlensing properties for a given star field. The first realistic light-curve simulations were carried out by Paczynski (1986), KRS and Schneider & Weiss (1987). In these papers, the authors assumed for simplicity that all stars in front of the quasar are of equal mass. Kayser et al.

(1989) computed light curves for star fields containing objects of different masses.

Microlensing is now well-understood theoretically, and there is already some observational evidence for it. The most exciting data are those of Corrigan et al. (1990, 1991) who detected differences between the lightcurves of the four components of the ‘‘Einstein cross’’ 2237+030 which must be a result of microlensing; however, the lightcurves are not sufficiently resolved in time and the measurement errors are relatively large. Vanderriest et al. (1989) tried to determine the time delay ΔT between the components A and B of the ‘‘Double Quasar’’ 0957+561 and found a probable value of $\Delta T = 415 \pm 20$ days. After shifting the B-lightcurve by ΔT there remained some differences which Vanderriest et al. interpreted in terms of microlensing. (There is also a difference in the A/B flux ratios between the radio, the emission lines and the optical continuum, which might be a result of microlensing.) Angonin et al. (1990) found differences in the equivalent widths and/or the profiles of the broad emission as well as the broad absorption lines between the four images of the ‘‘Clover Leaf’’ H 1413+117 and discussed this in terms of microlensing.

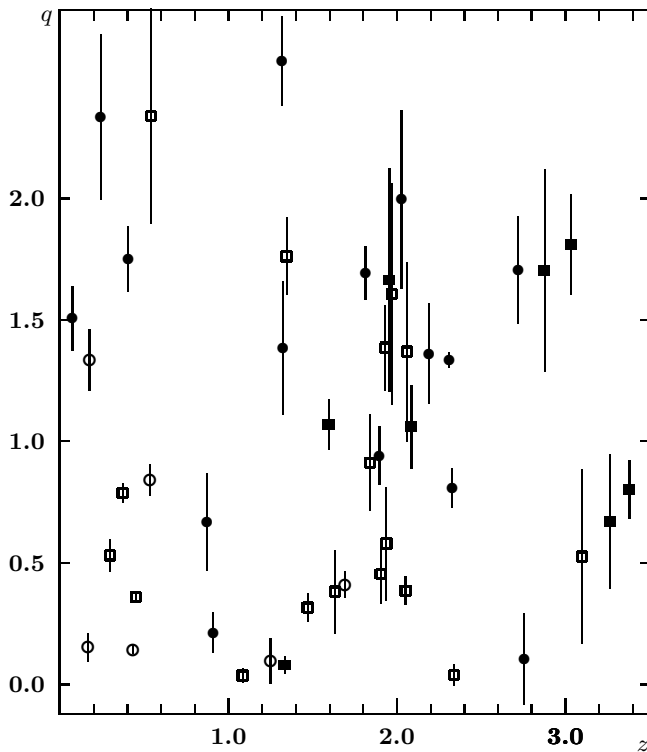


Fig. 6. Maximum variation relative to the average variation of the corresponding quasar sub-sample, q , versus redshift z . *Filled circles:* $G1$ -objects; *open circles:* $G2$ -objects; *open squares:* $A1$ -objects; *Filled squares:* other objects

The HQM quasar sample has been selected to include good candidates for microlensing variability. We did, however, not succeed in discovering a typical *high amplification event* (cf. KRS) in any of our lightcurves. All flares recorded up to now occurred in radio loud objects and were very probably of intrinsic origin (cf. the detailed discussion of the 3C 345 lightcurve in Schramm et al. 1993a). Thus, if microlensing is present in our sample it leads only to low amplitude variations. Such vari-

ations occur if the source is larger than the Einstein radii of the foreground stars; see, e.g., Refsdal & Stabell (1991). In this case the microlensing variations do not show a typical shape so that they can only be found statistically. In Fig. 6, we have plotted the variability index

$$q = R'_{\text{qso}} / \langle R'_{\text{qso}} \rangle \quad (4)$$

for each quasar. Our sample includes 14 $G1$ -objects for which we assume the highest microlensing probability; 9 of them are more strongly variable than the average in the corresponding sub-class. We regard this result as a statistical hint of microlensing. Note that there is no indication of enhanced variability for the $A1$ -objects. Only further observations and a better theoretical understanding of the intrinsic variability mechanisms may lead to a better knowledge on the importance of microlensing.

Acknowledgements. It would have been impossible to carry out our program without the excellent support by the MPIA and the Calar Alto staff members. We like to thank J. v. Linde, M.-D. Linnert, D. Mehlert, L. Nieser, M. Schaaf, T. Schramm and H.J. Witt for their help during lots of long and sometimes painful cold nights at Calar Alto and P. King and S. Refsdal for carefully reading the manuscript. This work has been supported by the Deutsche Forschungsgemeinschaft under Bo 904/1, Re 439/5 and Schr 292/6.

References

- Angel J.R.P., Stockman H.S., 1980, ARA&A 18, 321
 Angione R.J., 1973, AJ 78, 353, (A73)
 Angonin M.-C., Remy M., Surdej J., Vanderriest C., 1990, A&A 233, L5
 Arnaud J., Hammer F., Jones J., Le Fèvre O., 1988, A&A 206, L5
 Barbieri C., Romano G., Zambon M., 1979, A&AS 37, 551, (BRZ)
 Barthel P.D., Tytler D.R., Thomson B., 1990, A&AS 82, 339
 Bechtold J., Green R.F., Weymann R., Schmidt M., Estabrook F., Sherman R., Wahlquist D., Heckman T., 1984, ApJ 281, 76
 Bergeron J., 1988, in ‘QSO Absorption Lines – Probing the Universe’, ed. by J.C. Blades, D. Turnshek, C.A. Norman, Cambridge University Press, Cambridge, p. 127
 Bergeron J., Boulade O., Kundt D., Tytler D., Boksenberg A., Vigroux L., 1988, A&A 191, 1
 Blades J.C., 1988, in ‘QSO Absorption Lines – Probing the Universe’, ed. by J.C. Blades, D. Turnshek, C.A. Norman, Cambridge University Press, Cambridge, p. 147
 Blades J.C., Hunstead R.W., Murdoch H.S., 1981, MNRAS 194, 669
 Boissé P., Boulade O., 1990, A&A 236, 291
 Boksenberg A., Sargent W.L.W., 1978, ApJ 220, 42
 Borgeest U., Schramm K.-J., 1992. In: Kayser R., Schramm T., Nieser L. (eds.) Proc. Hamburg Conf. on ‘Gravitational Lensing’, Lecture Notes in Physics 406. Springer Verlag, Berlin, p. 164
 Borgeest U., 1986, ApJ 309, 467
 Borgeest U., Dietrich M., Hopp U., Kollatschny W., Schramm, K.-J., 1991a, A&A 243, 93, (BDHKS)

- Borgeest U., Kayser R., Refsdal S., Schramm K.-J., Schramm T., 1991b, in Lecture Notes in Physics #377, Proc. Heidelberg workshop on ‘Variability of Active Galaxies’, ed. by W.J. Duschl, S.J. Wagner, M. Camenzind, Berlin, p. 291
- Borgeest U., v. Linde J., Refsdal S., 1991c, A&A 251, L35
- Borgeest U., Refsdal, S. 1984, A&A 141, 318
- Borgeest U., Schramm K.-J., Refsdal S., 1990, Lecture Notes in Physics #360, Proc. Toulouse Workshop on ‘Gravitational Lensing’, ed. by Y. Mellier, B. Fort, G. Soucaïl, Springer-Verlag, Berlin, p. 203
- Bregman, 1990, A&AR 2, 125
- Bruhweiler F.C., Kafatos M., Sofia U.J., 1986, ApJ 303, L31
- Burbidge G., Smith H.E., Weymann R.A., Williams R.E., 1977, ApJ 218, 1
- Carswell R.F., Coleman G.D., Strittmatter P.A., Williams R.E., 1976, A&A 53, 275
- Chang K., Refsdal S., 1979, Nat 282, 561
- Chang K., Refsdal S., 1984, A&A 132, 168 (Erratum: 139, 558)
- Chen J.S., Morton D.C., Peterson B.A., Wright A.E., Jauncey D.L., 1981, MNRAS 196, 715
- Corrigan R.T., Irwin M.J., Arnaud J., Fahlman G.G., Fletcher J.M., Hewett P.C., Hewitt J.N., Le Fevre O., McClure R., Pritchett C.J., Schneider D.P., Turner E.L., Webster R.L., Yee H.K., 1991, AJ 102, 34
- Corrigan R.T., Irwin M.J., Hewett P.C., Webster R.L., 1990, Lecture Notes in Physics #360, Proc. Toulouse Workshop on ‘Gravitational Lensing’, ed. by Y. Mellier, B. Fort, G. Soucaïl, Springer-Verlag, Berlin, p. 206
- Crampton D., McClure R.D., Fletcher J.M., Hutchings J.B., 1989, preprint
- Cristiani S., 1987, A&A 175, L1
- Djorgovski S., McCarthy P., 1985, BAAS 17, 830
- Falco E.E., Gorenstein M., Shapiro I.I., 1991, ApJ 372, 364
- Foltz C., Chaffee F.H., Wolfe A.M., 1988, ApJ 335, 35
- Foltz C., Weymann R., Peterson B.M., Malkan M.A., Chaffee F.H., 1986, ApJ 307, 504
- Gott J.R., 1981, ApJ 243, 140
- Grandi S.A., Tift W.G., 1974, PASP 86, 873, (GT74)
- Heckman T.M., Bothun G.D., Balick B., 1984, AJ 89, 958
- Hewitt A., Burbidge G., 1987, ApJS 63, 1
- Hewitt A., Burbidge G., 1989, ApJS 69, 1
- Hutchings J.B., Hickson P., de Robertis M.M., 1986, AJ 92, 12
- Jenkins E., Caulet A., Wamsteker W., Blades J.C., Morton D., York D., 1987, in ‘QSO Absorption Lines’, ed. by J.C. Blades et al., STScI, p. 304
- Kayser R., Refsdal S., Stabell R., 1986, A&A 166, 36 (KRS)
- Kayser R., Weiss A., Refsdal S., Schneider P., 1989, A&A 214, 4
- Kühr H., McAlary C.W., Rudy R.J., Strittmatter P.A., Rieke G.H., 1984, ApJ 284, L5
- von Linde J., Borgeest U., Schramm K.-J., Graser U., Heidt J., Hopp U., Meisenheimer K., Nieser L., Steinle H., Wagner S.J., 1993, A&A 267, L23
- Linnert M.-D., 1992, diploma thesis, University of Hamburg
- Lloyd C., 1984, MNRAS 209, 697, (L84)
- Maccacaro T., Gioia I., Stocke J., 1984, ApJ 283, 486
- Magain P., Remy M., Surdej J., Swings J.-P., Smette A., 1990, Lecture Notes in Physics #360, Proc. Toulouse Workshop on ‘Gravitational Lensing’, ed. by Y. Mellier, B. Fort, G. Soucaïl, Springer-Verlag, Berlin, p. 57
- Maoz D., Bahcall J.N., Schneider D.P., Bahcall N.A., Djorgovski S., Doxsey R., Gould A., Kirhakos S., Meylan G., Yanny, B., 1993, ApJ 409, 28
- Miller J.S., Goodrich R.W., Stephens S.A., 1987, AJ 94, 633
- Moore P.K., Browne I.W.A., Daintree E.J., Noble R.G., Walsh D., 1981, MNRAS 197, 325
- Moore R.L., Stockman H.S., 1984, ApJ 279, 485, (MS84)
- Netzer H., Scheffer Y., 1983, MNRAS 203, 935, (NS83)
- Paczynski B., 1986, ApJ 301, 503
- Pica A.J., Pollock J.T., Smith A.G., Leacock R.J., Edwards P.L., Scott R.L., 1980, AJ 85, 1442, (PPSL)
- Pica A.J., Smith A.G., Pollock J.T., 1980, ApJ 238, 435
- Pica A.J., Smith A.G., 1983, ApJ 272, 11, (PS83)
- Pica A.J., Webb J.R., Smith A.G., Leacock R.J., Bitran M., 1987, AJ 94, 289
- Refsdal S., Stabell R., 1991, A&A 250, 62
- Reimers D., Clavel J., Groote D., Engels D., Hagen H.J., Naylor T., Wamsteker W., Hopp U. 1989, A&A 218, 71
- Rix H.-W., Hogan C.J., 1988, preprint
- Sargent W.L., Boksenberg A., Steidel C.C., 1988a, ApJS 68, 539
- Sargent W.L., Steidel C.C., 1990, ApJ 359, L37
- Sargent W.L., Steidel C.C., Boksenberg A., 1989, ApJS 69, 703
- Schneider P., Weiss A., 1987, A&A 171, 49
- Schramm K.-J., Borgeest U., 1992. In: Kayser R., Schramm T., Nieser L. (eds.) Proc. Hamburg Conf. on ‘Gravitational Lensing’, Lecture Notes in Physics 406. Springer Verlag, Berlin, p. 173
- Schramm K.-J., Borgeest U., Camenzind M., Wagner S.J., Bade N., Dreissigacker O., Heidt J., Hoff W., Kayser R., Kühl D., von Linde J., Linnert M.D., Pelt J., Schramm T., Sillanpää A., Takalo L.O., Valtaoja E., Vigotti M. 1993a, A&A, *in press*
- Schramm, K.-J., Borgeest U., Kühl D., von Linde J., Linnert M.D., 1993b, A&AS, *in press*, (Paper II)
- Schramm, K.-J., Borgeest U., Kühl D., von Linde J., Linnert M.D., 1993c, A&AS, *submitted*
- Selmes R.A., Tritton K.P., Wordsworth R.W., 1975, MNRAS 170, 17, (STW)
- Smith A.G., Nair A.D., Leacock R.J., Clement S.D., 1993, AJ 105, 437, (SNLC)
- Stocke J.T., Schneider P., Morris S.L., Gioia I.M., Maccacaro T., Schild R.E., 1987, ApJ 315, L11
- Stockton A.N. 1978, ApJ 223, 747
- Tritton K.P., Selmes R.A., 1971, MNRAS 153, 453, (TS71)
- Usher P.D., 1978, ApJ 222, 40
- Vanderriest C., Schneider J., Herpe G., Chevreton M., Moles M., Wlérick G., 1989, A&A 215, 1
- Véron-Cetty M.-P., Véron P., 1991, ESO scientific report # 10, (VV)
- Xie G.-z., Li K.h., Zhou Y., Lu R.-w., Wang J.-c., Cheng F.-z., Zhou Y.-y., Wu J.-x., 1988, AJ 96, 24
- Zamorani G., Giommi P., Maccacaro T., Tananbaum H., 1984, ApJ 278, 28